

Targeting Type 2 Diabetes with C-Glucosyl Dihydrochalcones as Selective Sodium Glucose Co-Transporter 2 (SGLT2) Inhibitors: Synthesis and Biological Evaluation

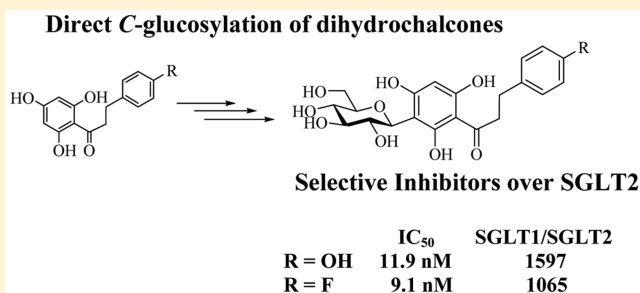
Ana R. Jesus,^{†,‡} Diogo Vila-Viçosa,[†] Miguel Machuqueiro,[†] Ana P. Marques,[†] Timothy M. Dore,^{*,‡,§} and Amélia P. Rauter^{*,†,§}

[†]Centro de Química e Bioquímica, Faculdade de Ciências, Universidade de Lisboa, Ed C8, Piso 5, Campo Grande, 1749-016 Lisboa, Portugal

[‡]New York University Abu Dhabi, P.O. Box 129188, Abu Dhabi, United Arab Emirates

Supporting Information

ABSTRACT: Inhibiting glucose reabsorption by sodium glucose co-transporter proteins (SGLTs) in the kidneys is a relatively new strategy for treating type 2 diabetes. Selective inhibition of SGLT2 over SGLT1 is critical for minimizing adverse side effects associated with SGLT1 inhibition. A library of C-glucosyl dihydrochalcones and their dihydrochalcone and chalcone precursors was synthesized and tested as SGLT1/SGLT2 inhibitors using a cell-based fluorescence assay of glucose uptake. The most potent inhibitors of SGLT2 (IC_{50} = 9–23 nM) were considerably weaker inhibitors of SGLT1 (IC_{50} = 10–19 μ M). They showed no effect on the sodium independent GLUT family of glucose transporters, and the most potent ones were not acutely toxic to cultured cells. The interaction of a C-glucosyl dihydrochalcone with a POPC membrane was modeled computationally, providing evidence that it is not a pan-assay interference compound. These results point toward the discovery of structures that are potent and highly selective inhibitors of SGLT2.



INTRODUCTION

Type 2 diabetes is a chronic metabolic disease in which hyperglycemia results mainly from the malfunction of insulin produced by β -cells in the pancreas.^{1–3} In diabetic subjects, hyperglycemia can lead to hyperfiltration of glucose, resulting in glucosuria (excretion of glucose through urine).⁴ Food digestion, glycogen breakdown, and gluconeogenesis provide glucose to the human body. Inhibition of glucose absorption in the intestine to treat type 2 diabetes is the mechanism of action of the well-known α -glucosidase inhibitors acarbose, miglitol, and voglibose.^{5–7} More recently, inhibition of glucose reabsorption in the kidneys has become a viable strategy for lowering blood sugar levels in patients with type 2 diabetes.^{8–11} On a daily basis, the renal glomerulus filters approximately 180 g of glucose, which is reabsorbed by the kidneys with >99% sugar reabsorption primarily in the proximal tubules^{12–14} by sodium glucose co-transporter proteins (SGLTs). There are six isoforms of SGLTs;^{4,15} SGLT1 and SGLT2 are the most well-known.^{16,17} SGLT1 is located in the small intestine, heart, trachea, and kidney and has a high affinity to both glucose and galactose, while the single substrate for SGLT2, located only in the kidneys, is glucose.^{4,18–20}

Phlorizin (1), a natural glucosylated dihydrochalcone found in the bark of apple trees, was the first SGLT inhibitor reported in the literature²¹ (Figure 1). However, it was found to cause

severe side effects in the gastrointestinal tract because it inhibits both SGLT1 and SGLT2, and its metabolite, phloretin, inhibits the glucose transporter GLUT1. Inhibition of the GLUT family of transporters is another possible source of adverse side effects. For these reasons and phlorizin's low oral bioavailability, it did not proceed to clinical trials.^{22,23} Pharmaceutical companies have modified phlorizin's structure to increase selectivity. For example, the methyl carbonate of 3-(benzofuran-5-yl)-1-[2-(β -D-glucopyranosyloxy)-6-hydroxy-4-methylphenyl]propan-1-one (T-109SA, 2)²⁴ is absorbed and subsequently metabolized into its active form. This compound has a 4-fold increase in the SGLT2/SGLT1 selectivity, yet similarly to phlorizin it also has poor bioavailability. The replacement of the O-glucosides by C-glucosyl analogs,^{23–29} which are stable to hydrolysis and resistant to endogenous hydrolases, leads to a longer half-life and duration of action.²⁸ Among those approved as drugs, canagliflozin (3), dapagliflozin (4a), and empagliflozin (4b) have high selectivity for SGLT2 over SGLT1, whereas others are still in clinical trials.^{4,13–15,20,25} Studies on the safety and efficacy of 3 and 4a show that these two drugs are safe in the short term, but long-term safety remains undetermined.^{26,30} Both drugs cause renal-related side effects, namely, hypoglycemia.

Received: July 29, 2016

Published: November 28, 2016



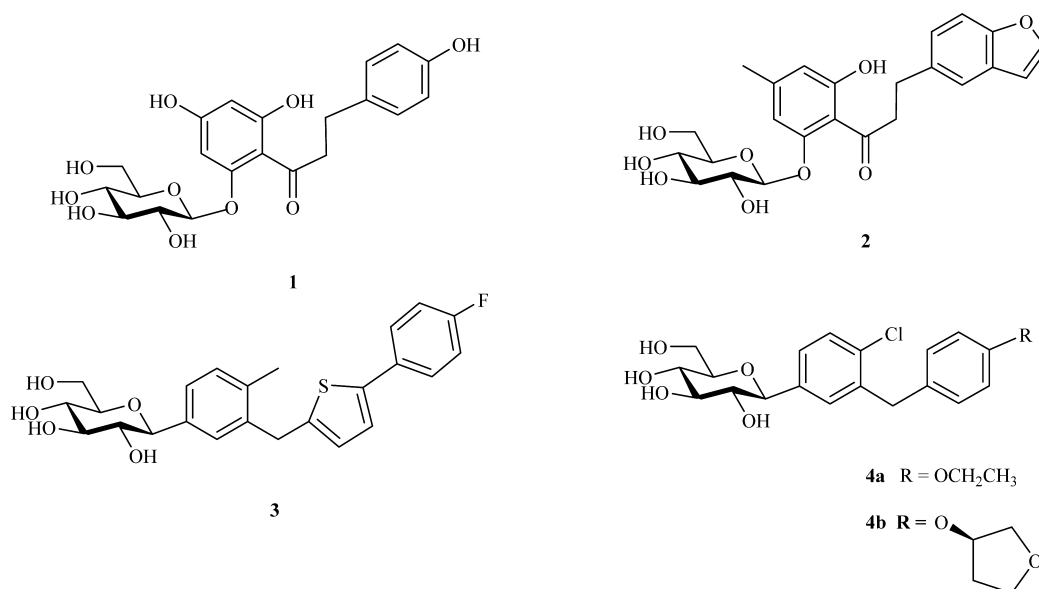
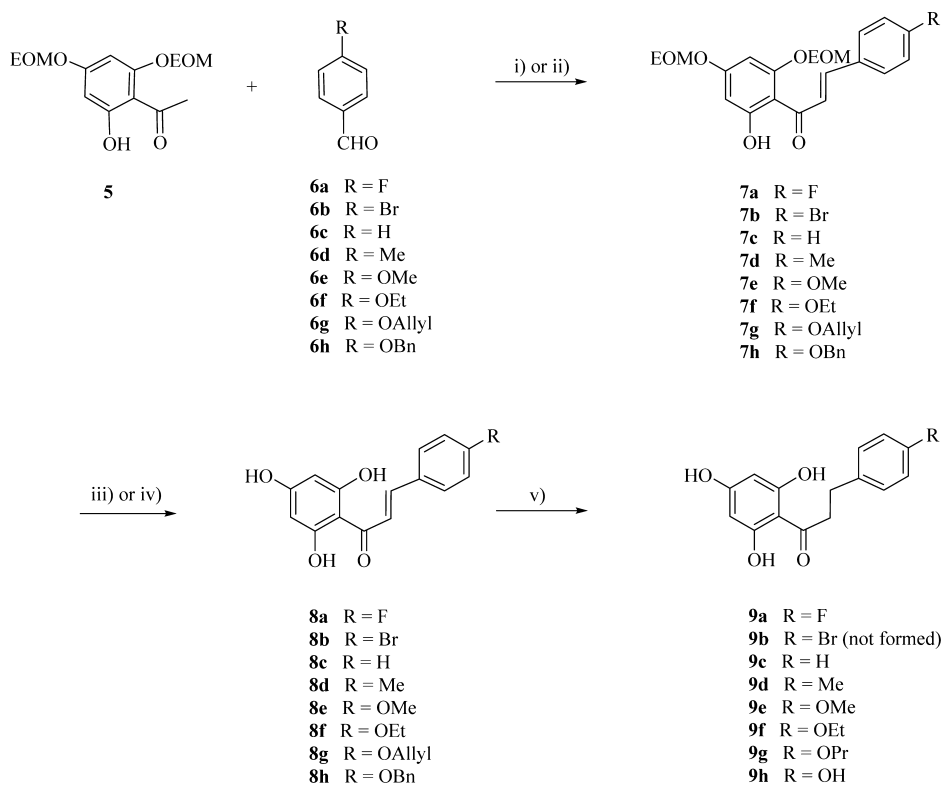


Figure 1. Structures of SGLT2 inhibitors phlorizin (1), phlorizin analogue 2, canagliflozin (3), dapagliflozin (4a), and empagliflozin (4b).

Scheme 1. Synthesis of 2',4',6'-Trihydroxychalcones and 2',4',6'-Trihydroxydihydrochalcones^a

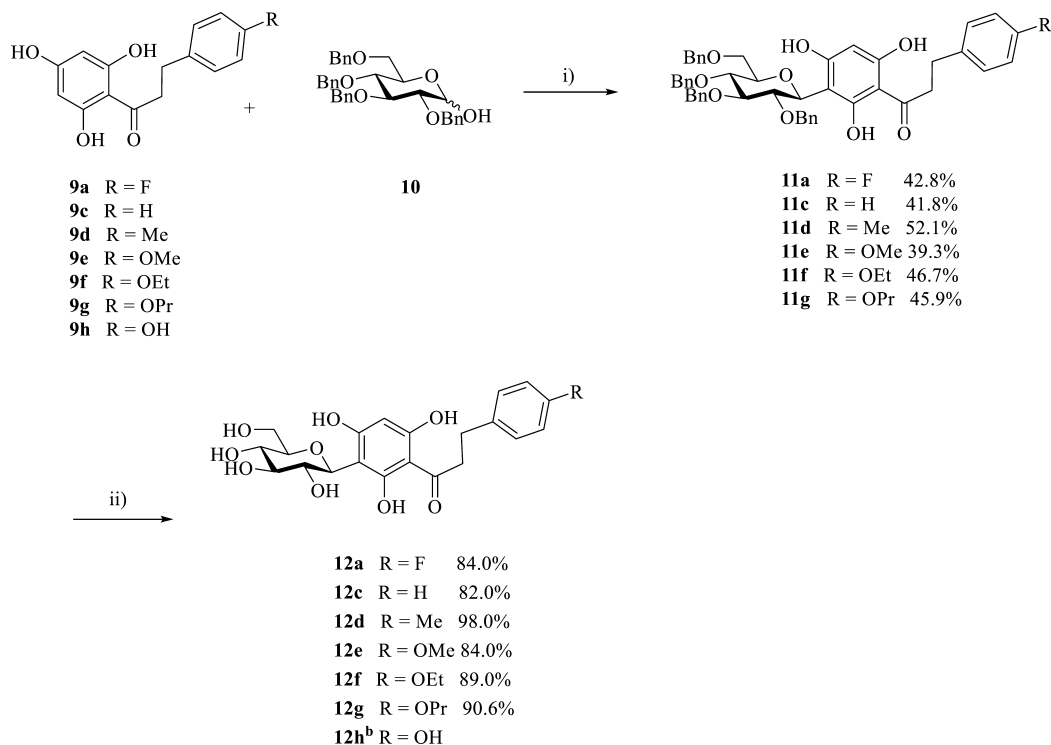


^aReagents and conditions: (i) 50% aq NaOH (w/v), EtOH, rt, 24 h; (ii) 50% aq NaOH (w/v), EtOH, 120 °C, 250 W, 1 h; (iii) FeCl₃·6H₂O, MeOH, reflux, 2–3 h; (iv) FeCl₃·6H₂O, MeOH, 80 °C, 7–10 min; (v) Et₃SiH, Pd/C, EtOAc, MeOH, rt, 10 min.

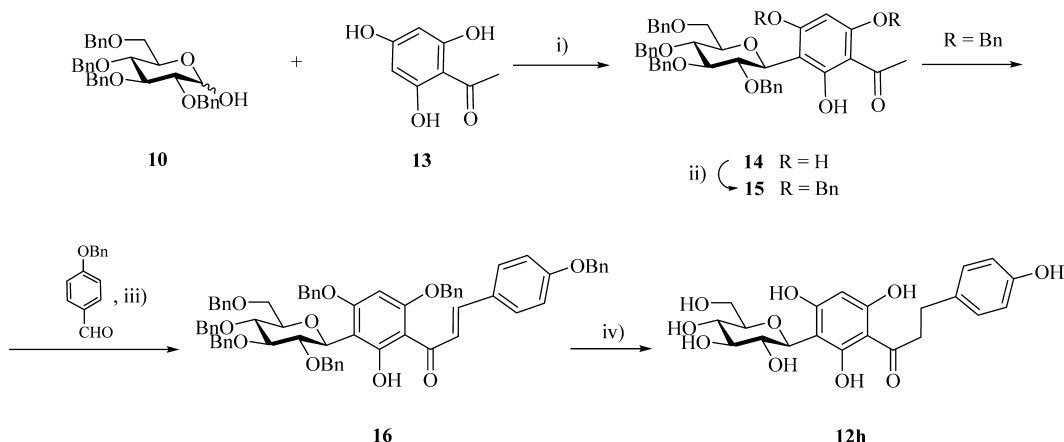
mic episodes, urinary tract infections, female genital mycotic infections, and nasopharyngitis.³⁰ Most of these side effects are related to SGLT1 inhibition. Although some of these drugs are highly selective for SGLT2 over SGLT1 (>2000-fold), new selective drugs toward SGLT2 over SGLT1 and GLUT transporters with fewer side effects could possibly be created by exploiting other synthetically accessible compound families.

C-Glucosyl dihydrochalcones are found in green rooibos (*Aspalathus linearis*) extracts, for which there is evidence of

antidiabetic activity.^{31,32} To further investigate the possible molecular mechanisms for this observation, we synthesized a small library of C-glucosyl dihydrochalcones (12a,c–h), their chalcone precursors (8a–h), and dihydrochalcone aglycones (9a,c–h) (Scheme 1). We also describe the first and successful use of triethylsilane and palladium on carbon for the selective alkene hydrogenation of the reported chalcones, in the presence of the carbonyl group. Whereas C-glucosylation of small phenols has been quite well investigated,^{33–42} we describe

Scheme 2. Synthesis of C-Glucosyl Dihydrochalcones^a

^aReagents and conditions: (i) TMSOTf, CH₂Cl₂, CH₃CN, Drierite, 0 °C, then rt, 2–5 h; (ii) Et₃SiH, Pd/C, EtOAc, MeOH, rt, 5 h. ^bFor reagents and conditions to prepare **12h**, see Scheme 3.

Scheme 3. Synthesis of Nothofagin (**12h**)^a

^aReagents and conditions: (i) TMSOTf, CH₂Cl₂, CH₃CN, Drierite, 0 °C, then rt, 5 h, 56%; (ii) BnBr, K₂CO₃, DMF, rt, 1.5 h, 74%; (iii) 50% aq NaOH (w/v), EtOH, reflux, 24 h, 63%; (iv) Et₃SiH, Pd/C, EtOAc, MeOH, rt, 5 h, 79%

here a new procedure for the C-glucosylation of unprotected dihydrochalcones that uses trimethylsilyl trifluoromethanesulfonate (TMSOTf) as a catalyst. The compounds were assessed for their ability to inhibit glucose uptake by human SGLT1 and SGLT2 in vitro using HEK293 cells stably expressing one or the other of the two proteins and for their impact on cell viability using an assay of metabolic capacity and on GLUT-based glucose transport. To ascertain the risk that the C-glucosyl dihydrochalcones were pan-assay interference compounds (PAINS),⁴³ especially those that modulate membranes and muddle the response of membrane receptors, we adapted a known computational protocol⁴⁴ to quantify the effects of one of the most active C-glucosyl dihydrochalcones

(nothofagin, **12h**) in a {(2*R*)-3-hexadecanoyloxy-2-[(*Z*)-octadec-9-enoyl]oxypropyl} 2-(trimethylazaniumyl)ethyl phosphate (POPC) model membrane.

RESULTS AND DISCUSSION

Chemistry. C-Glucosyl dihydrochalcones **12a,c–g** (Scheme 2) were prepared from the corresponding dihydrochalcones **9a,c–g** (Scheme 1) and 2,3,4,6-tetra-O-benzyl-D-glucopyranose (**10**). Nothofagin⁴⁵ (**12h**) was synthesized by a variation on the strategy (Scheme 3). Dihydrochalcones **9a,c–h** were synthesized starting from 1-[2,4-bis(ethoxymethoxy)-6-hydroxyphenyl]ethan-1-one (**5**) and *para*-substituted benzaldehydes **6a–h** in three steps. Aldol condensation of **5** with

aromatic aldehydes **6a–h** under basic conditions provided 2',4'-bis(ethoxymethoxy)-6'-hydroxychalcones **7a–h** in good yields (86–99%). Deprotection of **7a–h** in the presence of the Lewis acid $\text{FeCl}_3 \cdot 6\text{H}_2\text{O}$ afforded the 2',4',6'-trihydroxychalcones **8a–h** in 73–98% yield. These two steps were carried out with both microwave and conventional heating. The results (Table 1) show that microwave heating did not change the yield substantially, but the reaction time was decreased in both steps.

Table 1. Reaction Yields of Chalcone and Dihydrochalcone Synthesis

compd	yield (%) ^a	
	conventional	microwave
7a	92	98
7b	91	97
7c	95	96
7d	97	96
7e	87	91
7f	86	92
7g	99	99
7h	88	92
8a	88	97
8b	96	95
8c	80	82
8d	81	73
8e	80	83
8f	89	90
8g	82	89
8h	87	86
9a	98	
9b	-	
9c	94	
9d	99	
9e	97	
9f	96	
9g	94	
9h	97	

^aIsolated yield.

Addition of triethylsilane to a palladium-charcoal catalyst generated molecular hydrogen in situ, resulting in a rapid and high-yielding reduction of the chalcone double bond in **8a–h** to afford the corresponding dihydrochalcones **9a,c–h** (Scheme 1) in high yield (Table 1), except for the bromine derivative **8b**, which underwent reduction of the bromoaryl moiety, affording compound **9c** instead of **9b**. This bromine–hydrogen exchange has been observed in other hydrosilane-mediated reductions.⁴⁶ Nevertheless, this method efficiently generated molecular hydrogen in situ for the reduction of the carbon–carbon double bond in α,β -unsaturated compounds, avoiding the handling of H_2 bottles.

With C-glucosylation of dihydrochalcone **9a** using 2,3,4,6-tetra-*O*-benzyl-D-glucopyranose (**10**) as the glucosyl donor in the presence of 0.25 equiv of TMSOTf , the C-glucosyl dihydrochalcone **11a** was obtained in 12% yield (Scheme 2). Increasing the amount of the catalyst up to 0.50 equiv improved the yield of **11a** to 43%, whereas using 0.75 equiv led to the formation of secondary products. The C-glucosylation of dihydrochalcones **9c–g** was carried out using 0.50 equiv of TMSOTf , affording the protected C-glucosyl dihydrochalcones **11c–g** in moderate yield (Scheme 2). Removal of benzyl

groups from the glucosyl moiety led to the formation of the target C-glucosyl dihydrochalcones **12a,c–g** in 24–40% overall yield for the five steps.

Nothofagin (**12h**) was prepared following an approach based on our previous work,⁴² starting with the C-glucosylation of acetophloroglucinol (**13**) under the same conditions as described above, followed by benzylation, aldol condensation, and deprotection (Scheme 3). The yield for the four-step synthesis of **12h** was only 21% but this synthetic pathway can be considered an improvement over the complex eight-step synthesis by Minehan et al.⁴⁷

Biological Evaluation. The ability of compounds **1**, **4a**, **8a–h**, **9a,c–h**, and **12a,c–h** to inhibit glucose uptake in vitro was evaluated in HEK293 cells stably expressing the human SGLT1 or SGLT2 proteins. HEK293 cells were transfected with either a pCMV6-Neo-SGLT1 or a pCMV6-Neo-SGLT2 plasmid, and stably transfected clones were selected using G418, an analog of the antibiotic neomycin sulfate. The expression of SGLT1 or SGLT2 genes in stably transfected HEK293 cells was confirmed by reverse transcription PCR (RT-PCR) (Figure 2). Strong bands corresponding to the PCR

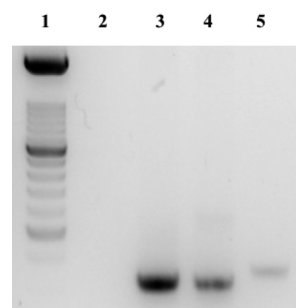


Figure 2. Expression of SGLT1 and SGLT2 in HEK293 cells by RT-PCR. Two bands of 328 and 321 bp are observed corresponding to SGLT1 and SGLT2 PCR products, respectively. Lane 1, 2.5 Kbp ladder; lane 2, nontransfected HEK293 cells; lane 3, pCMV6-Neo-SGLT1 transfected HEK293 cells; lane 4, pCMV6-Neo-SGLT2 transfected HEK293 cells; lane 5, nontransfected HEK293 cells.

products 328 bp for SGLT1 (lane 3) and 321 bp for SGLT2 (lane 5) in both cell lines were observed. No expression of SGLT1 and SGLT2 was observed in nontransfected HEK293 cells (lanes 2 and 5) used as negative control.

The overexpression of SGLT1 and SGLT2 proteins in the two stable HEK293 cell lines was confirmed by SDS–PAGE (Figure 3). Stronger bands in SGLT1 and SGLT2 stably transfected cells are observed (lanes 2 and 4, respectively) relative to nontransfected HEK293 cells (lanes 1 and 3).

The acute toxicity of compounds **1**, **8a–h**, **9a,c–h**, and **12a,c–h** was evaluated using a cell viability assay that assesses the metabolic capacity of cells. Nonviable cells lack metabolic capacity. After 20–24 h of incubation with the compounds at a concentration of 100 μM , the compounds showed no significant toxicity to HEK293 cells relative to untreated cells (Figure 4).

The glucose uptake in HEK293 cells stably expressing SGLT1 or SGLT2 proteins was measured by the methods described by Petty⁴⁸ and Minokoshi⁴⁹ with minor modifications. The method is based on the phosphorylation of 2-deoxyglucose (2DG) by endogenous hexokinase forming 2-deoxyglucose 6-phosphate (2DG6P), which is later oxidized by G6PDH in the presence of NADP^+ . The stoichiometrically

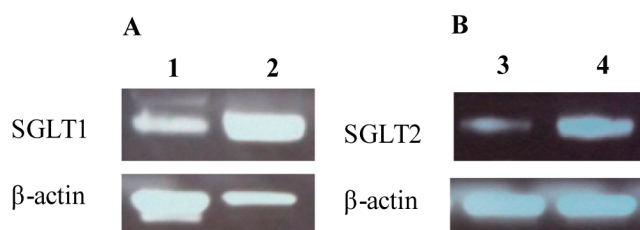


Figure 3. Immunoblot of SGLT1 and SGLT2 expression in stably transfected HEK293 cells: (A) lane 1, SGLT1 expression in nontransfected HEK293 cells; lane 2, SGLT1 expression in stable HEK293-SGLT1 cells; (B) lane 3, SGLT2 expression in nontransfected HEK293 cells; lane 4, SGLT2 expression in stable HEK293-SGLT2 cells. β -Actin was used as a loading control.

generated NADPH is then amplified by the diaphorase-resazurin cycling system to produce a highly fluorescent molecule, resofurin. The amount of resofurin formed is proportional to the amount of 2DG taken up by the cells and can be quantified using fluorescence spectroscopy. To confirm the viability of this assay for our system, the amount of 2DG taken up by HEK293 stably overexpressing either SGLT1 or SGLT2 and by nontransfected HEK293 cells was measured (Figure 5). We observed a greater than 2-fold increase in 2DG uptake in both stable cell lines compared to the control HEK293 cells. The 2DG uptake in the presence of compounds **1**, **4a**, **8a–h**, **9a,c–h**, and **12a,c–h** at a concentration of 100 μ M was measured in both stable cell lines and showed a complete inhibition of both SGLT1 and SGLT2 (Figure 6).

The IC_{50} values for the inhibition of glucose uptake by HEK293 cells stably transfected with SGLT1 or SGLT2 were measured independently (Table 2). Cells were treated with concentrations of compounds **1**, **4a**, **8a–h**, **9a,c–h**, and **12a,c–h** ranging from 0.1 nM to 200 μ M, and the level of glucose uptake was measured by the 2DG uptake assay. Phlorizin (**1**) and dapagliflozin (**4a**) were used as nonselective and selective SGLT2 inhibitors, respectively. Their IC_{50} values are 0.5 and 1.8 μ M, respectively, for SGLT1 and 67.3 and 0.8 nM, respectively, for SGLT2.

All of the synthesized C-glucosyl dihydrochalcones were potent inhibitors of SGLTs with at least 500-fold selectivity for SGLT2 over SGLT1. Inhibition of SGLTs by **12c** might explain its antihyperglycemic properties observed in rats.⁵⁰ The most

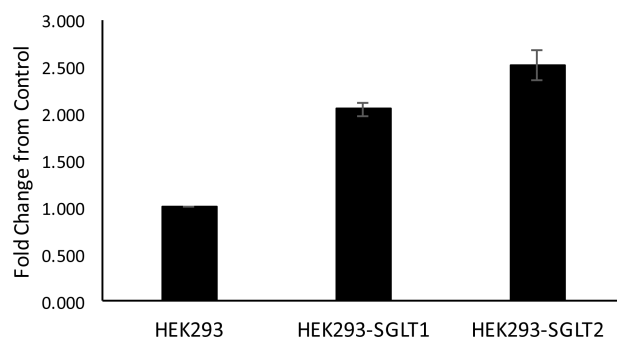


Figure 5. 2-Deoxyglucose uptake assay using HEK293 stably overexpressing either SGLT1 or SGLT2 and nontransfected HEK293 cells. Data are the mean \pm SD values from three independent experiments.

potent compounds against SGLT2 were **12a** (9.1 nM) and nothofagin (**12h**, 11.9 nM), the latter of which corroborates the results of computational docking studies using a homology model of SGLT2 that suggested nothofagin was an inhibitor of SGLT2.⁵¹ Compounds **12a** and **12h** were also the most selective for SGLT2 over SGLT1 (1065- and 1597-fold, respectively). The change from the O-glucoside, found in the nonselective SGLT inhibitor phlorizin (**1**), to the corresponding C-glucosyl derivative, nothofagin (**12h**), resulted in a 40-fold decrease in activity against SGLT1 and a nearly 6-fold increase in activity against SGLT2. Overall, **12h** is less active than dapagliflozin (**4a**) against SGLT2, and it is 10-fold less active against SGLT1 than **4a**.

To probe whether or not the C-glucosyl dihydrochalcone inhibitors of SGLT2 might also interfere with glucose transport through the GLUT family of transporters, the 2DG uptake assay was performed on the SGLT1 and SGLT2 stable cell lines in buffer lacking sodium by substituting choline chloride for sodium chloride. GLUT transporters are sodium independent, whereas SGLTs are sodium dependent. In the absence of sodium, GLUT transporters remain functional, whereas SGLTs do not transport glucose. When the 2DG uptake assay was performed in buffer lacking sodium, the C-glucosyl dihydrochalcones **12a,c–h** did not inhibit the uptake of glucose unless sodium was present, whereas all of the aglycones (chalcones and dihydrochalcones) inhibited glucose uptake regardless of whether sodium was present or not (Figure 7). In control

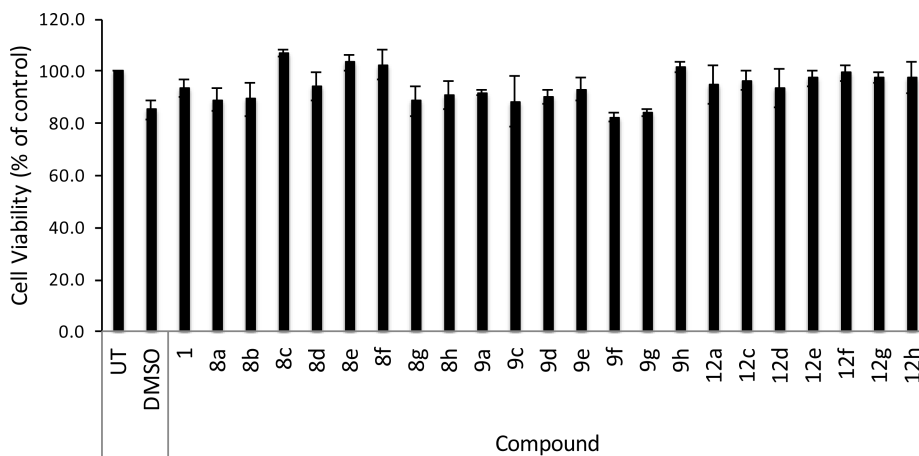


Figure 4. Cell viability assay applied to HEK293 cells using compounds **1**, **8a–h**, **9a,c–h**, and **12a,c–h**. Data are the mean \pm SD values from three independent experiments. The column labeled UT is untreated cells. DMSO was used as negative control.

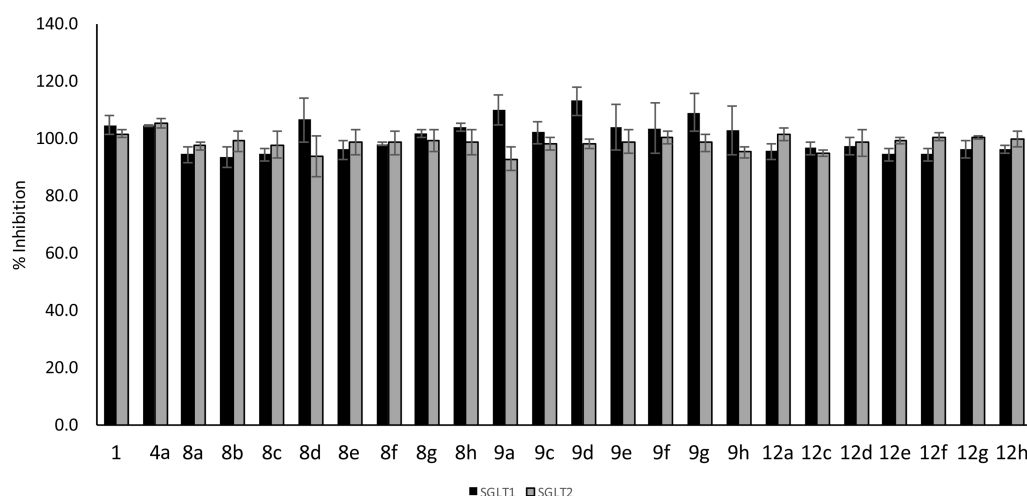


Figure 6. SGLT1 and SGLT2 inhibition at 100 μM compounds **1**, **4a**, **8a–h**, **9a,c–h**, and **12a,c–h**. Data are the mean \pm SD values from three independent experiments.

Table 2. IC_{50} Values of Compounds **1**, **4a**, **8a–h**, **9a,c–h**, and **12a,c–h** for SGLT1 and SGLT2

compd	IC_{50} (μM) ^a		selectivity SGLT1/SGLT2
	SGLT1	SGLT2	
1	0.499 \pm 0.120	0.0673 \pm 0.0051	7.4
4a	1.80 \pm 0.33	0.0008 \pm 0.0001	2250
8a	25.60 \pm 1.73	51.70 \pm 1.90	
8b	34.60 \pm 0.98	23.50 \pm 1.20	
8c	25.40 \pm 1.98	33.30 \pm 0.99	
8d	10.40 \pm 0.70	34.10 \pm 1.70	
8e	50.90 \pm 1.37	18.20 \pm 0.24	
8f	33.90 \pm 1.00	26.00 \pm 1.40	
8g	31.00 \pm 1.30	26.20 \pm 2.40	
8h	52.60 \pm 0.39	22.70 \pm 0.73	
9a	9.60 \pm 0.87	15.80 \pm 1.10	
9c	7.90 \pm 1.00	14.70 \pm 0.63	
9d	9.90 \pm 0.78	18.00 \pm 0.95	
9e	13.30 \pm 0.65	18.70 \pm 1.40	
9f	15.10 \pm 0.61	16.70 \pm 1.70	
9g	11.60 \pm 0.60	16.40 \pm 1.00	
9h	12.40 \pm 1.40	18.30 \pm 0.59	
12a	9.70 \pm 0.89	0.0091 \pm 0.0057	1065
12c	9.90 \pm 0.43	0.0198 \pm 0.0024	500
12d	10.60 \pm 0.89	0.0182 \pm 0.0020	582
12e	13.80 \pm 0.57	0.0213 \pm 0.0031	648
12f	14.60 \pm 0.10	0.0217 \pm 0.0044	673
12g	15.60 \pm 0.92	0.0227 \pm 0.0039	661
12h	19.00 \pm 1.3	0.0119 \pm 0.0026	1597

^aData are mean \pm SD values from three independent experiments.

experiments, cytochalasin B, a known inhibitor of GLUT transporters,^{52–54} inhibited glucose uptake in the absence and presence of sodium, whereas phlorizin (**1**), which is not known to inhibit GLUT transporters, did not inhibit glucose uptake in the absence of sodium. These results suggest that the C-glucosyl dihydrochalcones **12a,c–h** do not interfere with GLUT transporters.

There are online services that identify PAINS,^{55,56} however, their false discovery rate is significant because these tools are more oriented toward high-throughput screening. Andersen and co-workers developed a computational protocol to quantify the effects of several phytochemicals in a POPC membrane

model.⁴⁴ Their approach was based on potential of mean force (PMF) calculations in the absence and presence of the phytochemicals. By moving a 0.9 nm radius spherical probe across the different systems, the authors were able to estimate how the compounds alter the energy required to perturb the bilayer. In their results, curcumin, a known PAINS compound,⁴³ was found to have a strong effect, while resveratrol only had a mild effect.⁴⁴ We adapted this protocol⁴⁴ and performed the PMF calculations with an atomistic force field (GROMOS 54A7),⁵⁷ instead of the MARTINI force field,⁴⁴ which is coarse grained and less detailed. Figure 8 shows the PMFs for translocating a probe of radius ~ 0.6 nm across a pure POPC bilayer and binary mixtures of **12h** or resveratrol in POPC. In these PMF profiles, we observe a minimum of energy in the lipid tail region, which differs from the energy maximum that Andersen and co-workers observed.⁴⁴ This deviation probably results from the differing detail levels of the force fields used. Our profiles are in good agreement with the PMF reported for a methane-like sphere across a bilayer using an atomistic model.⁵⁸ Resveratrol, which is a mild PAINS compound according to a similar method,⁴⁴ seems to alter the energetics of membrane permeation in both the headgroup and center of the bilayer regions. Nothofagin (**12h**) only has a minor effect on the headgroup region, where it is concentrated, with no apparent perturbation of the remaining membrane. Therefore, it is unlikely that **12h** can act as a membrane modulator and present itself as a false positive in membrane protein assays, like other known PAINS.

CONCLUSION

C-Glucosyl dihydrochalcones were prepared by direct C-glucosylation of a series of unprotected dihydrochalcones, which were synthesized in high yield from 1-[2,4-bis-(ethoxymethoxy)-6-hydroxyphenyl]ethan-1-one (**5**) and *para*-substituted benzaldehydes (**6a–h**). The chalcones, dihydrochalcones, and C-glucosyl dihydrochalcones showed little toxicity to HEK293 cells in culture. At high concentration (100 μM), all of the compounds completely inhibited the glucose uptake in HEK293 cells stably expressing SGLT1 or SGLT2 proteins, but the C-glucosyl dihydrochalcones were particularly potent against SGLT2 (IC_{50} = 9–23 nM). The C-glucosyl dihydrochalcones demonstrated significantly high selectivity toward SGLT2 over SGLT1, but they were not

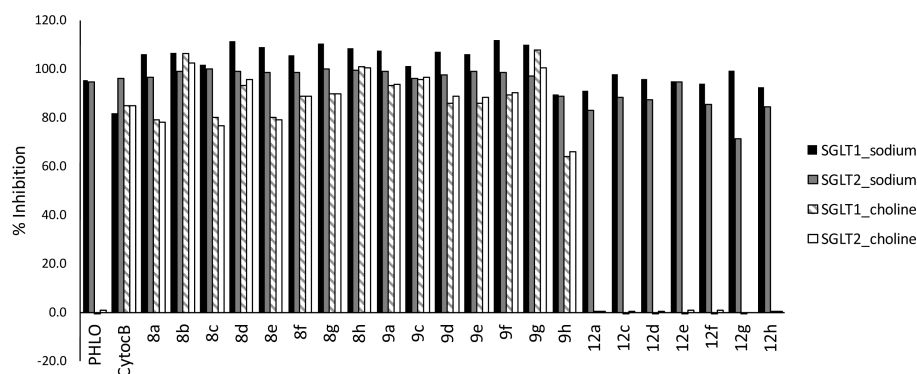


Figure 7. 2DG assay performed in sodium and choline buffer. The concentration of chalcones **8a–h**, dihydrochalcones **9a,c–h**, and C-glucosyl dihydrochalcones **12a,c–h** was 100 μ M. Phlorizin (PHLO) and cytochalasin B (CytoCB) were used as negative and positive controls, respectively.

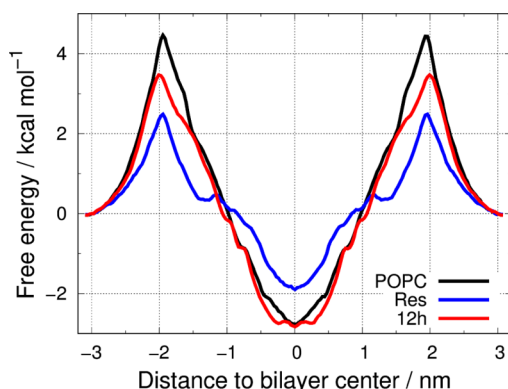


Figure 8. Symmetrized PMF for translocating a probe of radius ~ 0.6 nm across a POPC bilayer. The bilayer normal is set to the X-axis with zero at the center of the bilayer. POPC is the pure lipid bilayer, **12h** is nothofagin, and **Res** is resveratrol. For profiles with error bars, see [Supporting Information](#).

more selective than dapagliflozin (**4a**), which is currently on the market for the treatment of type 2 diabetes. Nevertheless, the C-glucosyl dihydrochalcones were all less active than dapagliflozin (**4a**) toward SGLT1. Inhibition of SGLT1 is thought to be the cause of some adverse side effects of SGLT inhibitors, including dapagliflozin (**4a**). The C-glucosyl dihydrochalcones **12a,c–h** appear to be inactive against the non-sodium dependent GLUT family of glucose transporters, another potential source of adverse side effects. The computational PMF profile of **12h** provides evidence that the C-glucosyl dihydrochalcones are not PAINS and suggests that the glucosyl group plays an important role in preventing deep membrane insertion. These results also show the importance of C-glucosylation to achieve higher selectivity for SGLT2 over SGLT1 and GLUT, by comparison to those obtained for phlorizin, the O-glucosyl analog.

EXPERIMENTAL SECTION

Chemistry. Solvents and reagents were obtained from commercial sources and used without further purification. Solutions were concentrated below 50 $^{\circ}$ C under vacuum on rotary evaporators. Qualitative TLC was performed on precoated 0.50 μ m silica gel 60 plates with a UV indicator; compounds were detected by UV light (254 nm) and spraying with a 10% methanol solution of sulfuric acid or with a 5% ethanol solution of iron(III) chloride hexahydrate followed by heating. Column chromatography was carried out on silica gel (40–60 μ m). NMR spectra were recorded at 400.13 MHz for 1 H NMR and 100.62 MHz for 13 C NMR. Chemical shifts are given in

ppm relative to tetramethylsilane. Assignments were made, when needed, with the help of COSY, HMQC, and HMBC experiments. Protons and carbons in ring A (aromatic ring nearest to the glucosyl group) are assigned as H', C'; in ring B (aromatic ring furthest from the glucosyl group) as H'', C''; and those belonging to the glucosyl moiety as H''', C''' to facilitate the description of the corresponding chemical shifts, while those belonging to the propanone moiety are assigned as C, H. HRMS spectra were acquired in an FTICR mass spectrometer equipped with a dual ESI/MALDI ion source and a 7 T actively shielded magnet. 1 H NMR data confirmed compound purity of $\geq 95\%$.

General Procedure for the Synthesis of Protected C-Glucosyl Dihydrochalcones. Under a N_2 atmosphere, a solution of dihydrochalcone **9** (2 equiv) in acetonitrile (2 mL) was added to a solution of 2,3,4,6-tetra-O-benzyl-D-glucopyranose (**10**) (1.23 mmol) in dichloromethane (10 mL) at room temperature. Drierite (200 mg) was added, and the reaction vessel was maintained under N_2 . The mixture was cooled to -30 $^{\circ}$ C, and TMSOTf (0.5 equiv) was added dropwise. After 20–30 min the reaction was allowed to reach room temperature. The total consumption of the glycosyl donor was confirmed by TLC (1:1 hexane/acetone), and after 2–5 h the reaction was quenched with a saturated aqueous solution of $NaHCO_3$. Drierite was removed by filtration through Celite, and the residue was extracted with dichloromethane. The extracts were washed with brine, dried over anhydrous $MgSO_4$, and concentrated to an oil, which was purified by column chromatography (7:1 hexane/acetone).

3-(4-Fluorophenyl)-1-[3-(2,3,4,6-tetra-O-benzyl- β -D-glucopyranosyl)-2,4,6-trihydroxyphenyl]propan-1-one (11a**).** Yield 43%; $R_f = 0.58$ (3:1 hexane/EtOAc). 1 H NMR ($CDCl_3$, 400 MHz, δ): 14.30 (2H, s, OH2', OH6'); 9.72 (1H, s, OH4'); 7.37–6.95 (24H, m, ArH, H2'', H3'', H5'', H6''); 6.01 (1H, s, H5'); 4.98 (2H, s, -OCH₂Ph); 4.88–4.86 (3H, m, -OCH₂Ph, H1'''); 4.73, 4.29 (2H, parts A and B of AB system, $J = 10.7$ Hz, -OCH₂Ph); 4.57, 4.48 (2H, parts A and B of AB system, $J = 9.2$ Hz, -OCH₂Ph); 4.57, 4.48 (2H, parts A and B of AB system, $J = 9.2$ Hz, -OCH₂Ph); 3.90–3.60 (6H, m, H2''', H3''', H4''', H5''', H6a''', H6b'''); 3.28–4.24 (2H, m, H2); 2.95 (2H, t, $J = 7.21$ Hz, H3). 13 C NMR ($CDCl_3$, 100 MHz, δ): 204.8 (C1); 162.5 (C2', C6'); 160.1 (C4', C4''); 136.8 (C1'); 138.2, 137.7, 137.3, 137.2 (C_q-Ph); 129.8 (C2'', C6'', $J_{CF} = 7.8$ Hz); 128.7, 128.6, 128.5, 128.3, 128.0, 127.8, 127.6 (CH-Ph); 115.0 (C3'', C5'', $J_{CF} = 21.4$ Hz); 86.2 (C2'''); 78.7 (C3'''); 76.2 (C4'''); 75.7 (C5'''); 75.3 (-OCH₂Ph); 75.1 (C1'''); 75.0, 74.6, 73.4 (-OCH₂Ph); 67.7 (C6''); 45.9 (C2); 29.6 (C3). HRMS-ESI (m/z): $[M + Na]^+$ calcd for $C_{49}H_{47}FO_9$ 821.30963; found, 821.30943.

3-Phenyl-1-[3-(2,3,4,6-tetra-O-benzyl- β -D-glucopyranosyl)-2,4,6-trihydroxyphenyl]propan-1-one (11c**).** Yield 42%; $R_f = 0.19$ (3:1 hexane/acetone). 1 H NMR ($CDCl_3$, 400 MHz, δ): 7.35–6.98 (25H, m, PhH, H2'', H3'', H4'', H5'', H6''); 5.96 (1H, s, 1H, H5'); 4.95 (2H, s, -OCH₂Ph); 4.85 (1H, d, $J = 8.7$ Hz, H1'''); 4.83, 4.51 (2H, parts A and B of AB system, $J = 11.0$ Hz, -OCH₂Ph); 4.69, 4.27 (2H, parts A and B of AB system, $J = 10.0$ Hz, -OCH₂Ph); 4.55, 4.46 (2H, parts A and B of AB system, $J = 11.3$ Hz, -OCH₂Ph); 3.86–3.58 (6H,

m, H2'', H3'', H4'', H5'', H6a'', H6b''); 3.30–3.26 (2H, m, H2); 2.97 (2H, t, $J = 8.9$ Hz, H-3). ^{13}C NMR (CDCl_3 , 100 MHz, δ): 205.0 (C1); 141.8 (C1''); 138.2, 137.7, 137.3, 136.2 ($\text{C}_q\text{-Ph}$); 128.7, 128.5, 128.4, 128.3, 128.0, 127.9, 127.8, 127.6 (CH-Ph , C2'', C3'', C5'', C6''); 125.9 (C4''); 106.0 (C3'); 102.8 (C1'); 99.9 (C5'); 86.2 (C2'''); 78.7 (C3'''); 77.2 (C4''); 76.3 (C5'''); 75.7 ($-\text{OCH}_2\text{Ph}$); 75.3 (C1'''); 75.2, 75.0, 73.4 ($-\text{OCH}_2\text{Ph}$); 67.5 (C6''); 45.9 (C2); 30.5 (C3). HRMS-ESI (m/z): $[\text{M} + \text{Na}]^+$ calcd for $\text{C}_{49}\text{H}_{48}\text{O}_9$ 803.31905; found 803.32129.

3-(4-Methylphenyl)-1-[3-(2,3,4,6-tetra-O-benzyl- β -D-glucopyranosyl)-2,4,6-trihydroxyphenyl]propan-1-one (11d). Yield 52%; $R_f = 0.60$ (3:1 hexane/EtOAc). ^1H NMR (CDCl_3 , 400 MHz, δ): 14.03 (2H, s, OH2', OH6'); 9.87 (1H, s, 1H, OH4'); 7.34–6.97 (24H, m, ArH, H2'', H3'', H5'', H6''); 5.89 (1H, s, H5'); 4.95, 4.91 (2H, parts A and B of AB system, $J = 10.0$ Hz, $-\text{OCH}_2\text{Ph}$); 4.87 (1H, d, $J = 10.0$ Hz, H1''); 4.83 (1H, $J = 8.5$ Hz, part A of AB system AB of $-\text{OCH}_2\text{Ph}$); 4.62, 4.21 (2H, parts A and B of AB system, $J = 10.6$ Hz, $-\text{OCH}_2\text{Ph}$); 4.57–4.47 (3H, m, part B system AB of $-\text{OCH}_2\text{Ph}$, parts A and B of AB system of $-\text{OCH}_2\text{Ph}$); 3.80–3.59 (6H, m, H2'', H3'', H4'', H5'', H6a'', H6b''); 3.27 (2H, t, $J = 7.4$ Hz, H2); 2.97 (2H, t, H3); 2.92 (3H, s, $-\text{CH}_3$ 4''). ^{13}C NMR (CDCl_3 , 100 MHz, δ): 205.2 (C1); 138.8 (C1''); 138.3, 137.8, 137.1, 136.4 ($\text{C}_q\text{-Ph}$); 135.4 (C4''); 129.1, 128.7, 128.6, 128.5, 128.4, 128.2, 128.1, 128.0, 127.8, 127.7 (CH-Ph , C2'', C3'', C5'', C6''); 105.7 (C3'); 102.5 (C1'); 97.5 (C5'); 86.2 (C2'''); 81.7 (C3'''); 78.3 (C4''); 77.3 (C5'''); 76.1 (C1'''); 75.7, 75.3, 74.9, 73.5 ($-\text{OCH}_2\text{Ph}$); 67.9 (C6''); 46.1 (C2); 30.1 (C3). HRMS-ESI (m/z): $[\text{M} + \text{Na}]^+$ calcd for $\text{C}_{50}\text{H}_{50}\text{O}_9$ 817.33478; found 817.33552.

3-(4-Methoxyphenyl)-1-[3-(2,3,4,6-tetra-O-benzyl- β -D-glucopyranosyl)-2,4,6-trihydroxyphenyl]propan-1-one (11e). Yield 39%; $R_f = 0.19$ (1:1 hexane/acetone). ^1H NMR (CDCl_3 , 400 MHz, δ): 14.43 (2H, s, OH2', OH6'); 7.33–7.12 (20H, m, ArH); 6.98 (2H, d, $J = 7.8$ Hz, H2'', H6''); 6.82 (2H, d, H3'', H5''); 5.89 (1H, s, H5'); 4.96–4.88 (3H, m, parts A and B of system AB of $-\text{OCH}_2\text{Ph}$, H1''); 4.82 (1H, part A of system AB of $-\text{OCH}_2\text{Ph}$); 4.59, 4.20 (2H, parts A and B of AB system, $J = 8.9$ Hz, $-\text{OCH}_2\text{Ph}$); 4.55–4.46 (3H, m, part B of system AB of $-\text{OCH}_2\text{Ph}$, parts A and B of AB system); 3.80–3.59 (10H, m, H2'', H3'', H4'', H5'', H6a'', H6b'', $-\text{OCH}_3$ 4''); 3.27 (2H, t, $J = 7.3$ Hz, H2); 2.93 (2H, t, H3). ^{13}C NMR (CDCl_3 , 100 MHz, δ): 205.2 (C1); 138.4, 137.7, 137.1, 136.6 ($\text{C}_q\text{-Ph}$); 133.9 (C1''); 129.5 (C2'', C6''); 128.7, 128.6, 128.5, 128.1, 128.0, 127.7 (CH-Ph); 113.8 (C3'', C5''); 105.6 (C3'); 102.5 (C1''); 97.3 (C5'); 86.2 (C2'''); 81.1 (C3'''); 78.8 (C4''); 77.4 (C5'''); 76.0 (C1'''); 75.8, 75.3, 74.8, 73.5 ($-\text{OCH}_2\text{Ph}$); 68.0 (C6''); 55.3 ($-\text{OCH}_3$ 4''); 46.2 (C2); 31.9 (C3). HRMS-ESI (m/z): $[\text{M} + \text{Na}]^+$ calcd for $\text{C}_{50}\text{H}_{50}\text{O}_{10}$ 833.32962; found 833.33521.

3-(4-Ethoxyphenyl)-1-[3-(2,3,4,6-tetra-O-benzyl- β -D-glucopyranosyl)-2,4,6-trihydroxyphenyl]propan-1-one (11f). Yield 47%; $R_f = 0.16$ (1:1 hexane/acetone). ^1H NMR (CDCl_3 , 400 MHz, δ): 7.32–7.11 (20H, m, ArH); 6.98 (2H, d, $J = 7.6$ Hz, H2'', H6''); 6.81 (2H, d, H3'', H5''); 5.92 (1H, s, H5'); 4.97–4.82 (4H, m, parts A and B of system AB of $-\text{OCH}_2\text{Ph}$, part A of system AB of $-\text{OCH}_2\text{Ph}$, H1''); 4.63, 4.22 (2H, parts A and B of system A, $J = 10.3$ Hz, $-\text{OCH}_2\text{Ph}$); 4.56–4.55 (3H, m, part B of system AB of $-\text{OCH}_2\text{Ph}$, parts A and B of system AB of $-\text{OCH}_2\text{Ph}$); 4.00 (2H, q, $J = 7.4$ Hz, $J = 13.1$ Hz, $-\text{OCH}_2\text{CH}_3$ 4''); 3.81–3.59 (6H, m, H2'', H3'', H4'', H5'', H6a'', H6b''); 3.28–3.24 (2H, m, H2); 2.91 (2H, t, $J = 7.6$ Hz, H3); 1.40 (3H, t, $-\text{OCH}_2\text{CH}_3$ 4''). ^{13}C NMR (CDCl_3 , 100 MHz, δ): 205.2 (C1); 157.1 (C4''); 138.3, 137.7, 137.2, 136.4 ($\text{C}_q\text{-Ph}$); 133.8 (C1''); 129.4 (C2'', C6''); 128.7, 128.5, 128.4, 128.1, 128.0, 127.8, 127.6 (CH-Ph); 114.4 (C3'', C5''); 105.7 (C3'); 102.6 (C1'); 97.5 (C5'); 86.2 (C2'''); 81.9 (C3'''); 78.7 (C4''); 77.2 (C5'''); 76.1 (C1'''); 67.8 (C6''); 75.7, 75.3, 74.9, 73.4 ($-\text{OCH}_2\text{Ph}$); 63.4 ($-\text{OCH}_2\text{CH}_3$ 4''); 46.2 (C2); 29.7 (C3); 14.9 ($-\text{OCH}_2\text{CH}_3$ 4''). HRMS-ESI (m/z): $[\text{M} + \text{Na}]^+$ calcd for $\text{C}_{51}\text{H}_{52}\text{O}_{10}$ 847.34527; found 847.34662.

3-(4-Propyloxyphenyl)-1-[3-(2,3,4,6-tetra-O-benzyl- β -D-glucopyranosyl)-2,4,6-trihydroxyphenyl]propan-1-one (11g). Yield 46%; $R_f = 0.18$ (1:1 hexane/acetone). ^1H NMR (CDCl_3 , 400 MHz, δ): 14.03 (s, 2H, OH2', OH6'); 7.34–7.12 (20H, m, ArH); 6.98 (2H, d, $J = 6.8$ Hz, H2'', H6''); 6.82 (2H, d, H3'', H5''); 5.93 (1H, s, H5'); 4.96, 4.92 (2H, parts A and B of system AB, $-\text{OCH}_2\text{Ph}$); 4.88

(1H, d, $J = 9.6$ Hz, H1''); 4.83 (1H, part A of system AB, $J = 10.5$ Hz, $-\text{OCH}_2\text{Ph}$); 4.65, 4.24 (2H, parts A and B of system AB, $J = 10.3$ Hz, $-\text{OCH}_2\text{Ph}$); 4.56–4.45 (3H, m, parts A and B of system AB, part B of system AB of $-\text{OCH}_2\text{Ph}$); 3.89 (2H, t, $J = 6.9$ Hz, $-\text{OCH}_2\text{CH}_2\text{CH}_3$ 4''); 3.82–3.60 (6H, m, H2'', H3'', H4'', H5'', H6a'', H6b''); 3.30–3.18 (2H, m, H2); 2.91 (2H, t, $J = 7.1$ Hz, H3); 1.79 (2H, q, $J = 14.1$ Hz, $J = 20.4$ Hz, $-\text{OCH}_2\text{CH}_2\text{CH}_3$ 4''); 1.03 (3H, t, $-\text{OCH}_2\text{CH}_2\text{CH}_3$ 4''). ^{13}C NMR (CDCl_3 , 100 MHz, δ): 205.2 (C1); 157.3 (C4''); 138.3, 137.7, 137.3, 136.7 ($\text{C}_q\text{-Ph}$); 133.7 (C1''); 129.4 (C2'', C6''); 128.7, 128.5, 128.4, 128.2, 128.1, 128.0, 127.9, 127.8, 127.6 (CH-Ph); 114.4 (C3'', C5''); 105.8 (C3'); 102.7 (C1'); 97.7 (C5'); 86.2 (C2'''); 81.7 (C3'''); 78.7 (C4''); 77.2 (C5'''); 76.2 (C1''); 69.5 (C6''); 75.7, 75.3, 74.9, 73.4 ($-\text{OCH}_2\text{Ph}$); 67.7 ($-\text{OCH}_2\text{CH}_2\text{CH}_3$ 4''); 46.2 (C2); 29.7 (C3); 22.7 ($-\text{OCH}_2\text{CH}_2\text{CH}_3$ 4''); 10.6 ($-\text{OCH}_2\text{CH}_2\text{CH}_3$ 4''). HRMS-ESI (m/z): $[\text{M} + \text{Na}]^+$ calcd for $\text{C}_{52}\text{H}_{54}\text{O}_{10}$ 861.36092; found 861.36124.

General Procedure for the Synthesis of C-Glucosyl Dihydrochalcones. Compound 11 or 16⁴² (0.5 mmol) was dissolved in EtOAc (1 mL) and methanol (2 mL). The 5% Pd/C catalyst was added under a N_2 atmosphere followed by dropwise addition of triethylsilane (10 equiv); effervescence was observed, indicating that hydrogen was being formed in situ. The reaction was maintained at room temperature until TLC confirmed completion (5 h). The catalyst was removed by filtering the reaction mixture through Celite. The volume of solvent in the filtrate was reduced to one-third under vacuum, and most of the triethylsilane was removed by extraction (three times) with acetonitrile/hexane (1:1). The final product was purified by column chromatography (EtOAc only).

3-(4-Fluorophenyl)-1-[3-(β -D-glucopyranosyl)-2,4,6-trihydroxyphenyl]propan-1-one (12a). Yield 84%; mp 80.2–80.7 °C; $R_f = 0.36$ (7:1 $\text{CH}_2\text{Cl}_2/\text{MeOH}$). ^1H NMR (acetone- d_6 , 400 MHz, δ): 7.33 (2H, dd, $J_{\text{H,H}} = 8.37$ Hz, $J_{\text{H,F}} = 5.2$ Hz, H2'', H6''); 7.05 (2H, t, $J_{\text{H,F}} = 8.7$ Hz, H3'', H5''); 5.95 (1H, s, H5'); 4.94 (1H, d, $J = 9.6$ Hz, H1''); 3.91–3.83 (2H, m, H6a'', H6b''); 3.67 (2H, t, $J = 9.0$ Hz, H2'', H3''); 3.58 (1H, t, $J = 9.2$ Hz, H4''); 3.50 (1H, ddd, $J = 9.6$ Hz, $J = 6.1$ Hz, $J = 3.0$ Hz, H5''); 3.39 (2H, t, $J = 7.3$ Hz, H2); 2.98 (2H, t, H3). ^{13}C NMR (acetone- d_6 , 100 MHz, δ): 204.5 (C1'); 163.0 (C4'); 162.4 (C2', C6'); 160.0 (C4''); 138.0, 137.9 (C1''); 130.2, 130.1 (C2'', C6''); 114.9, 114.7 (C3'', C5''); 104.5 (C3'); 103.4 (C1'); 95.6 (C5'); 81.1 (C5''); 78.3 (C4''); 75.4 (C1''); 73.3 (C3''); 69.6 (C2''); 60.9 (C6''); 45.9 (C2); 29.7 (C3). HRMS-ESI (m/z): $[\text{M} + \text{Na}]^+$ calcd for $\text{C}_{21}\text{H}_{23}\text{FO}_9$ 461.12183; found 461.12238.

1-[3-(β -D-Glucopyranosyl)-2,4,6-trihydroxyphenyl]-3-phenylpropan-1-one (12c). Yield 82.0%; mp 80.0–80.1 °C; $R_f = 0.40$ (7:1 $\text{CH}_2\text{Cl}_2/\text{MeOH}$). ^1H NMR (acetone- d_6 , 400 MHz, δ): 12.20 (1H, s, OH6'); 11.50 (1H, s, OH2'); 9.10 (1H, s, OH4'); 7.30–7.26 (4H, m, H2'', H3'', H5'', H6''); 7.21–7.17 (1H, m, H4''); 5.95 (1H, s, H5'); 4.94 (1H, d, $J = 9.7$ Hz, H1''); 3.91–3.81 (2H, m, H6a'', H6b''); 3.70–3.62 (2H, m, H2'', H3''); 3.58–3.46 (2H, m, H4'', H5''); 3.40 (2H, t, $J = 7.7$ Hz, H2); 2.99 (2H, t, H3). ^{13}C NMR (acetone- d_6 , 100 MHz, δ): 205.5 (C1); 163.0 (C2', C4', C6'); 141.9 (C1''); 128.5 (C2'', C6''); 128.3 (C3'', C5''); 125.8 (C4''); 104.5 (C3'); 103.8 (C1'); 95.6 (C5'); 81.1 (C5''); 78.7 (C4''); 75.4 (C1''); 73.3 (C3''); 69.9 (C2''); 60.7 (C6''); 45.8 (C2); 30.4 (C3). HRMS-ESI (m/z): $[\text{M} + \text{Na}]^+$ calcd for $\text{C}_{21}\text{H}_{24}\text{O}_9$ 443.13125; found 443.13169.

1-[3-(β -D-Glucopyranosyl)-2,4,6-trihydroxyphenyl]-3-(4-methylphenyl)propan-1-one (12d). Yield 82.0%; mp 117.0–117.5 °C; $R_f = 0.38$ (7:1 $\text{CH}_2\text{Cl}_2/\text{MeOH}$). ^1H NMR (acetone- d_6 , 400 MHz, δ): 7.19 (2H, d, $J = 7.2$ Hz, H2'', H6''); 7.11 (2H, d, H3'', H5''); 5.96 (1H, s, H5'); 4.95 (1H, d, $J = 9.1$ Hz, H1''); 3.91–3.84 (6H, m, H6a'', H6b''); 3.67 (2H, t, $J = 9.1$ Hz, H2'', H3''); 3.58 (1H, t, $J = 9.0$ Hz, H4''); 3.50 (1H, ddd, $J = 9.5$ Hz, $J = 6.6$ Hz, $J = 2.9$ Hz, H5''); 3.38 (2H, t, $J = 6.9$ Hz, H2); 2.95 (2H, t, H3); 2.30 (3H, s, $-\text{CH}_3$ 4''); (acetone- d_6 , 100 MHz, δ): 204.8 (C1); 163.2 (C2', C6'); 163.0 (C4'); 138.9 (C1''); 134.9 (C4''); 128.9 (C2'', C6''); 128.2 (C3'', C5''); 104.5 (C3'); 103.4 (C1'); 95.6 (C5'); 81.1 (C5''); 78.4 (C4''); 75.4 (C1''); 73.4 (C3''); 69.6 (C2''); 60.7 (C6''); 45.9 (C2); 30.0 (C3); 20.5 ($-\text{CH}_3$ 4''). HRMS-ESI (m/z): $[\text{M} + \text{Na}]^+$ calcd for $\text{C}_{22}\text{H}_{26}\text{O}_9$ 457.14690; found 457.14758.

1-[3-(β -D-Glucopyranosyl)-2,4,6-trihydroxyphenyl]-3-(4-methoxyphenyl)propan-1-one (12e). Yield 84.0%; mp 90.4–90.7 °C; R_f = 0.31 (7:1 CH₂Cl₂/MeOH); ¹H NMR (acetone-*d*₆, 400 MHz, δ): 12.29 (2H, s, OH2', OH6'); 11.57 (1H, s, OH4'); 9.17 (1H, s, OH4''); 7.21 (2H, d, J = 7.7 Hz, H2'', H6''); 6.85 (2H, d, H3'', H5''); 5.94 (1H, s, H5'); 4.94 (1H, d, J = 9.7 Hz, H1'''); 3.91–3.87 (6H, m, H6a'', H6b''); 3.77 (3H, s, -OCH₃4''); 3.66 (2H, t, J = 9.0 Hz, H2'', H3''); 3.56 (1H, t, J = 8.7 Hz, H4'''); 3.50 (1H, ddd, J = 9.9 Hz, J = 6.7 Hz, J = 3.3 Hz, H5'''); 3.36 (2H, t, J = 7.6 Hz, H2); 2.92 (2H, t, H3). ¹³C NMR (acetone-*d*₆, 100 MHz, δ): 205.3 (C1); 162.9 (C2', C4', C6'); 158.0 (C4''); 133.8 (C1''); 129.4 (C2'', C6''); 113.7 (C3'', C5''); 104.5 (C3'); 104.5 (C1'); 95.6 (C5'); 81.1 (C5''); 78.4 (C4''); 75.4 (C1''); 73.4 (C3''); 69.6 (C2''); 60.6 (C6''); 54.5 (-OCH₃4''); 46.2 (C2); 29.5 (C3). HRMS-ESI (m/z): [M + Na]⁺ calcd for C₂₂H₂₆O₁₀ 473.14182; found 473.14245.

3-(4-Ethoxyphenyl)-1-[3-(β -D-glucopyranosyl)-2,4,6-trihydroxyphenyl]propan-1-one (12f). Yield 89.0%; mp 91.4–92.0 °C; R_f = 0.10 (EtOAc). ¹H NMR (acetone-*d*₆, 400 MHz, δ): 12.36 (1H, s, OH6'); 11.45 (1H, s, OH2''); 9.11 (1H, s, OH4'); 7.17 (2H, d, J = 8.2 Hz, H2'', H6''); 6.82 (2H, d, H3'', H5''); 5.94 (1H, s, H5'); 4.93 (1H, d, J = 9.7 Hz, H1'''); 3.99 (2H, q, J = 7.2 Hz, J = 13.3 Hz, -OCH₂CH₃4''); 3.89–3.86 (6H, m, H6a'', H6b''); 3.72–3.47 (4H, m, H2'', H3'', H4'', H5''); 3.33 (2H, t, J = 9.4 Hz, H2); 2.89 (2H, t, H3); 1.34 (3H, t, -OCH₂CH₃4''). ¹³C NMR (acetone-*d*₆, 100 MHz, δ): 204.9 (C1); 163.1 (C2', C6'); 163.0 (C4''); 157.3 (C4''); 133.7 (C1''); 129.4 (C2'', C6''); 114.3 (C3'', C5''); 104.5 (C3'); 103.1 (C1'); 95.6 (C5'); 81.1 (C5''); 78.4 (C4''); 75.3 (C1''); 73.3 (C3''); 69.7 (C2''); 62.9 (-OCH₂CH₃4''); 60.8 (C6''); 46.1 (C2); 29.6 (C3); 14.3 (-OCH₂CH₃4''). HRMS-ESI (m/z): [M + Na]⁺ calcd for C₂₃H₂₈O₁₀ 487.15747; found 487.15789.

1-[3-(β -D-Glucopyranosyl)-2,4,6-trihydroxyphenyl]-3-(4-propyloxyphenyl)propan-1-one (12g). Yield 90.6%; mp 80.0–80.2 °C; R_f = 0.10 (EtOAc). ¹H NMR (acetone-*d*₆, 400 MHz, δ): 7.11 (2H, d, J = 7.6 Hz, H2'', H6''); 6.85 (2H, d, H3'', H5''); 5.95 (1H, s, H5'); 4.94 (1H, d, J = 8.8 Hz, H1'''); 3.94–3.90 (2H, m, -OCH₂CH₂CH₃4''); 3.89–3.83 (6H, m, H6a'', H6b''); 3.66 (2H, t, J = 9.3 Hz, H2'', H3''); 3.58–3.49 (2H, m, H4'', H5''); 3.36 (2H, t, J = 7.6 Hz, H2); 2.92 (2H, t, H3); 1.81–1.73 (2H, m, -OCH₂CH₂CH₃4''); 1.02 (3H, t, -OCH₂CH₂CH₃4''). ¹³C NMR (acetone-*d*₆, 100 MHz, δ): 204.8 (C1); 162.9 (C2', C4', C6'); 157.5 (C4''); 133.7 (C1''); 129.3 (C2'', C6''); 114.3 (C3'', C5''); 104.5 (C3'); 103.4 (C1'); 95.6 (C5''); 81.1 (C5''); 78.5 (C4''); 75.4 (C1''); 73.3 (C3''); 69.6 (C2''); 69.1 (-CH₂CH₂CH₃4''); 60.6 (C6''); 40.2 (C2); 29.7 (C3); 22.4 (-CH₂CH₂CH₃4''); 9.9 (-CH₂CH₂CH₃4''). HRMS-ESI (m/z): [M + Na]⁺ calcd for C₂₄H₃₀O₁₀ 501.17312; found 501.17373.

1-[3-(β -D-Glucopyranosyl)-2,4,6-trihydroxyphenyl]-3-(4-hydroxyphenyl)propan-1-one (12h). Yield 78.8%; mp 133.3–133.4 °C; R_f = 0.26 (7:1 CH₂Cl₂/MeOH). ¹H NMR (acetone-*d*₆, 400 MHz, δ): 7.11 (2H, d, J = 8.0 Hz, H2'', H6''); 6.75 (2H, d, H3'', H5''); 5.96 (1H, s, H5'); 4.94 (1H, d, J = 9.6 Hz, H1'''); 3.90–3.83 (2H, m, H6a'', H6b''); 3.30–3.64 (2H, m, H2'', H3''); 3.56 (1H, t, J = 8.9 Hz, H4''); 3.50 (1H, ddd, J = 9.6 Hz, J = 6.6 Hz, J = 3.1 Hz, H5''); 3.34 (2H, t, J = 7.3 Hz, H2); 2.88 (2H, t, H3). ¹³C NMR (acetone-*d*₆, 100 MHz, δ): 204.9 (C1'); 163.1 (C2', C4'); 162.9 (C6'); 155.5 (C4''); 132.5 (C1''); 129.4 (C2'', C6''); 115.1 (C3'', C5''); 104.5 (C3'); 103.4 (C1'); 81.1 (C5''); 78.5 (C4''); 75.4 (C1''); 73.3 (C3''); 69.6 (C2''); 60.6 (C6''); 46.3 (C2); 29.7 (C3). HRMS-ESI (m/z): [M + Na]⁺ calcd for C₂₁H₂₄O₁₀ 459.12617; found 459.12664.

Biological Evaluation. 2-Deoxy-D-glucose (2DG), 2-deoxy-D-glucose 6-phosphate sodium salt, hexokinase (from *Saccharomyces cerevisiae*), glucose 6-phosphate dehydrogenase (G6PDH, from *Leuconostoc mesenteroides*), resazurin sodium salt, triethanolamine (TEA) buffer, HEPES, β -nicotinamide adenine dinucleotide phosphate (β -NADP⁺), adenosine 5'-triphosphate disodium salt (ATP), phlorizin, cytochalasin B, diaphorase (from *Clostridium kluyveri* type II-L), bovine serum albumin (BSA), potassium chloride, sodium deoxycholate, choline chloride, fetal bovine serum (FBS), Dulbecco's modified Eagle medium (DMEM), Geneticin (G418), phosphate buffered saline, 2-[N-(7-nitrobenz-2-oxa-1,3-diazol-4-yl)amino]-2-de-

oxyglucose (2-NBDG), and dapagliflozin (4a) were purchased from commercial sources.

Cell Culture. Human embryonic kidney cells (HEK293) were obtained from the American Type Culture Collection (ATCC). HEK293 cells were grown in DMEM supplemented with 10% FBS and maintained at 37 °C in a 5% CO₂ atmosphere.

Cell Viability Assay. HEK293 cells were placed in a 96-well plate at a density of 2.0×10^4 cells/well 24 h prior to the assay. Each compound (1, 8a–h, 9a–h, 12a,c–h) was added at a concentration of 100 μ M in triplicate and incubated for 20–24 h at 37 °C in a 5% CO₂ atmosphere. Cells treated with DMSO were used as a positive control. CellTiter-Blue (20 μ L) was added to each well and incubated at 37 °C for 4 h. Fluorescence was measured in a microplate reader (λ_{ex} = 560 nm, λ_{em} = 590 nm). Cell viability was calculated as a ratio of fluorescence emission of treated vs nontreated cells and reported as a percentage.

Preparation of pCMV6-Neo Plasmids Containing hSGLT1 or hSGLT2. DH5 α cells were transformed with vectors containing human SGLT1 and SGLT2 complementary DNAs (cDNAs) (pCMV6-Neo, Origene), plated on Luria–Bertani (LB) agar plates impregnated with ampicillin, and incubated overnight at 37 °C. After 24 h of incubation, two colonies were picked and grown further in LB broth containing ampicillin at 37 °C overnight. pCMV6-Neo vectors containing SGLT1 and SGLT2 cDNA, respectively, were isolated and purified from the DH5 α cells using a PureLink HiPure Plasmid Filter Maxiprep kit (Sigma). The purity and concentration of each plasmid were confirmed by using a nanodrop spectrometer before use.

SGLT1 and SGLT2 Stable Cell Lines. HEK293 cells were plated on three 35 mm dishes at a density of 4.0×10^5 cells/dish and incubated at 37 °C overnight. Each of two dishes was transfected with either of the SGLT1 or SGLT2 plasmids using Truefect. The third dish was treated with only TrueFect as a control. Cells were trypsinized 24 h post-transfection and plated on a 24-well plate at a density of 8.0×10^4 cells/well. G418 was added to each well (700 μ g/mL) 48 h post-transfection. The medium including fresh antibiotic was replaced every 2 days for 7 days. After this period, the concentration of G418 was reduced to 300 μ g/mL and the clones were allowed to grow for several weeks until sufficiently confluent for cryopreservation.

RNA Isolation and Reverse Transcription PCR. Stably transfected SGLT1 or SGLT2 cells were plated on 35 mm dishes at 4.0×10^5 cells/dish and incubated at 37 °C overnight. Total RNA of each clone was isolated using a High Pure RNA isolation kit (Roche 11828665001). Reverse transcriptase reactions were performed using SuperScript VILO cDNA Synthesis Kit (Invitrogen) for first-strand cDNA synthesis. Polymerase chain reaction (PCR) was performed using Taq DNA polymerase (Invitrogen). The primers used were designed using Primer-3 Software. The primers for SGLT1 were 5'-TCCACTCATTTTGGCATTCA-3' (forward) and 5'-AAACCAACCCCTGCTGACATC-3' (reverse). The primers for SGLT2 were 5'-AGAGCCTGACCCACATCAAG-3' (forward) and 5'-GCGTGTA-GATGTCCATGGTG-3' (reverse). The RT-PCR was carried out in a thermal cycler using the following conditions: 94 °C for 2 min, 30 cycles of 94 °C for 30 s, 60 °C for 30 s, 72 °C for 1 min, then 72 °C for 5 min, hold at 4 °C. Agarose gel electrophoresis was used to separate PCR-amplified products, which were visualized under UV light.

Western Blot. Cells were plated on 60 mm dishes at 6.0×10^5 cells/dish and incubated at 37 °C overnight. Cells were lysed, and 50 μ g of each lysate was separated by sodium dodecyl sulfate polyacrylamide gel (SDS–PAGE). After electrophoresis, proteins were transferred to nitrocellulose membranes and then blocked with 10% milk in TBST (20 mM Tris, pH 7.6, 140 mM NaCl, and 0.1% Tween 20) for 75 min. The membranes were washed with TBST and subsequently incubated with a primary antibody to SGLT1 (1:200, H-85 Santa Cruz Biotechnology) or SGLT2 (1:500, H-45 Santa Cruz Biotechnology) in 5% BSA for 75 min at room temperature. β -Actin was used as a loading control, and the membrane was incubated with the corresponding primary antibody (1:1000, no. 4967, Cell Signaling). After washing the membranes with TBST, they were incubated with anti-rabbit horseradish peroxidase-conjugated second-

dary antibody (1:2000 for SGLT1 and β -actin and 1:4000 for SGLT2) for 1 h at room temperature. The signal was detected by chemoluminescence using an enhanced chemiluminescence (ECL) detection system.

2-Deoxyglucose Uptake Assay. HEK293 and SGLT1/SGLT2-transfected cells were plated at 2.0×10^4 cells/well in a 96-well plate. After 24 h of incubation, the culture medium was removed, and cells were rinsed once with Krebs–Ringer-phosphate-HEPES (KRPH) buffer and incubated in KRPH buffer for 1 h at 37 °C. 2-Deoxyglucose (1 mM) was added to each well and the cells were incubated at 37 °C for 1 h, after which cells were lysed with 50 μ L of 0.1 M NaOH followed by incubation at 80–85 °C for 40 min. The lysate was neutralized with 50 μ L of 0.1 M HCl, and 50 μ L of TEA buffer was added. In a 96-well plate, 100 μ L of lysate was dispensed into each well and incubated at 37 °C for 15–20 h after the addition of an enzymatic cocktail solution containing 50 mM TEA at pH 8.2, 50 mM KCl, 0.02% BSA, 1 mM NADP, 0.5 U/mL G6PDH, 0.1 U/mL diaphorase, 10 μ M resazurin. Fluorescence was measured at 590 nm using a plate reader upon excitation at 560 nm. The fluorescence intensity of resofurin, the reduced form of resazurin, correlates to the amount of 2DG inside the cells.

Determination of IC_{50} . To determine the IC_{50} values of compounds **1**, **4a**, **8a–h**, **9a,c–h**, and **12a,c–h**, HEK293, SGLT1, and SGLT2-transfected cells were plated at 2.0×10^4 cells/well in a 96-well plate. After 24 h of incubation, the culture medium was removed and cells were rinsed once with KRPH buffer and incubated in KRPH buffer for 1 h at 37 °C. Each compound (0.1 nM to 200 μ M) was added to the buffer and incubated for 10 min. 2-Deoxyglucose (1 mM) was added to each well and the cells were incubated at 37 °C for 1 h. Cells were lysed with 50 μ L of 0.1 M NaOH and then incubated at 80–85 °C for 40 min. The lysate was neutralized with 50 μ L of 0.1 M HCl, and 50 μ L of TEA buffer was added. The enzymatic assay to determine the amount of 2DG was performed as described above.

Computations. All molecular dynamics simulations were performed with the GROMOS 54A7 force field⁵⁷ using GROMACS 5.1.2⁵⁹ with the single point charge (SPC) water model.⁶⁰ The force-field parameters for nothofagin (**12h**) and resveratrol were obtained from an automated topology builder (ATB) server.⁶¹ A twin-range cutoff was used with short- and long-range cutoffs of 8 and 14 Å, respectively, and with neighbor lists updated every five steps. Long-range electrostatic interactions were treated with the reaction-field method⁶² using a dielectric constant of 54. The lipid and compound bond lengths were constrained using the P-LINCS algorithm,⁶³ while the SETTLE algorithm was used for water.⁶⁴ The time step used was 2 fs. The temperature of the systems was separately coupled to a γ -rescale temperature bath at 310 K and with relaxation times of 0.1 ps.⁶⁵ A semi-isotropic Parrinello–Rahman pressure coupling⁶⁶ was used at 1 bar with a relaxation time of 5 ps and a compressibility of 4.5×10^{-5} bar⁻¹. Three systems were built: pure POPC, resveratrol/POPC in a 12:128 ratio, and nothofagin/POPC also in a 12:128 ratio. The three systems were equilibrated for 50 ns prior to execution of the potential of mean force (PMF) calculations.

We determined the PMF associated with the diffusion process across a POPC bilayer of a Lennard-Jones (LJ) particle. This procedure was adapted from the literature, where the authors use a coarse grain force field.⁴⁴ The particle can be seen as a probe and was built analogously to a benzene molecule, with $C6 = 1.01 \times 10^{-1}$ kJ mol⁻¹ nm⁶, $C12 = 2.14 \times 10^{-2}$ kJ mol⁻¹ nm¹², and a mass of 78 Da. For each pre-equilibrated system, we built 32 initial structures for the umbrellas by placing the LJ particle in different positions, ranging from the center of the bilayer (0 nm) to a distance of 3.1 nm (in intervals of 0.1 nm), corresponding to bulk water. Each umbrella was 50 ns long, and the last 45 ns were used in the PMF calculation. All PMF profiles were calculated using weighted histogram analysis method (WHAM)⁶⁷ as implemented in GROMACS, and the Bayesian histogram bootstrapping was performed using 50 bootstrap iterations. The zero energy was set to 3 nm for representation convenience.

■ ASSOCIATED CONTENT

Supporting Information

The Supporting Information is available free of charge on the ACS Publications website at DOI: 10.1021/acs.jmedchem.6b01134.

Detailed protocols for the synthesis of compounds **8a–h** and **9a,c–h**; NMR spectra for all compounds; HRMS spectra for compounds **11a,c–g** and **16**; IC_{50} curves of compounds **1**, **4a**, **8a–h**, **9a,c–h**, and **12a,c–h**; PMFs with error bars; and compound characterization check list (PDF)

Molecular formula strings (CSV)

■ AUTHOR INFORMATION

Corresponding Authors

*T.M.D.: e-mail, timothy.dore@nyu.edu; phone, (+971) 2 628 4762.

*A.P.R.: e-mail, aprauter@fc.ul.pt; phone, (+351) 217 500 952 or (+351) 964 408 824.

ORCID

Timothy M. Dore: 0000-0002-3876-5012

Amélia P. Rauter: 0000-0003-3790-7952

Notes

The authors declare no competing financial interest.

■ ACKNOWLEDGMENTS

We thank the European Union's Seventh Framework Programme for Research, Technological Development, and Demonstration for funding the Diagnostic and Drug Discovery Initiative for Alzheimer's Disease (Grant 612347, 2014–2018) and the Fundação para a Ciência e a Tecnologia (FCT) for providing financial support to the project (UID/MULTI/00612/2013), the Ph.D. fellowship for A.R.J. (Grant SFRH/BD/78236/2011), the BPD fellowship for M.M. (Grant SFRH/BPD/110491/2015), and the acquisition of the equipment used to collect HRMS data (Grant REDE/1501/REM/2005). We also thank Paulo Costa for fruitful discussions on computational modeling. The biological research was carried out using Core Technology Platform resources at New York University Abu Dhabi.

■ ABBREVIATIONS USED

SGLT, sodium glucose co-transporter; GLUT, glucose facilitative transporter; EOM, ethoxymethyl; PAINS, pan-assay interference compounds; PMF, potential of mean force

■ REFERENCES

- (1) American Diabetes Association.. Diagnosis and Classification of Diabetes Mellitus. *Diabetes Care* **2004**, 27 (Suppl. 1), S5–S10.
- (2) Kitabchi, A. E.; Umpierrez, G. E.; Miles, J. M.; Fisher, J. N. Hyperglycemic Crises in Adult Patients with Diabetes. *Diabetes Care* **2009**, 32, 1335–1343.
- (3) Landin-Olsson, M. Latent Autoimmune Diabetes in Adults. *Ann. N. Y. Acad. Sci.* **2002**, 958, 112–116.
- (4) Su, S.-L. Sodium-Glucose Transporter. *Formosan J. Endocrinol. Metab.* **2009**, 1, 1–5.
- (5) van de Laar, F. A.; Lucassen, P. L.; Akkermans, R. P.; van de Lisdonk, E. H.; Rutten, G. E.; van Weel, C. α -Glucosidase Inhibitors for Patients with Type 2 Diabetes: Results from a Cochrane Systematic Review and Meta-Analysis. *Diabetes Care* **2005**, 28, 154–163.
- (6) Ahr, H. J.; Boberg, M.; Krause, H. P.; Maul, W.; Mueller, F. O.; Ploschke, H. J.; Weber, H.; Wuensche, C. Pharmacokinetics of

Acarbose. Part I. Absorption, Concentration in Plasma, Metabolism and Excretion after Single Administration of [^{14}C]Acarbose to Rats, Dogs and Man. *Arzneim.-Forsch.* **1989**, *39*, 1254–1260.

(7) Ahr, H. J.; Boberg, M.; Brendel, E.; Krause, H. P.; Steinke, W. Pharmacokinetics of Miglitol. Absorption, Distribution, Metabolism, and Excretion Following Administration to Rats, Dogs, and Man. *Arzneim.-Forsch.* **1997**, *47*, 734–745.

(8) Kinne, R. K. H.; Castaneda, F. SGLT Inhibitors as New Therapeutic Tools in the Treatment of Diabetes. In *Diabetes: Perspectives in Drug Therapy*; Schwanstecher, M., Ed.; Springer: Heidelberg, Germany, 2011; Vol. 203, pp 105–126, DOI: [10.1007/978-3-642-17214-4_5](https://doi.org/10.1007/978-3-642-17214-4_5).

(9) Ceriello, A. PROactive Study: (R)Evolution in the Therapy of Diabetes? *Diabetic Med.* **2005**, *22*, 1463–1464.

(10) Asano, N. Glycosidase Inhibitors: Update and Perspectives on Practical Use. *Glycobiology* **2003**, *13*, 93R–104R.

(11) Borges de Melo, E.; Gomes, A. d. S.; Carvalho, I. α - and β -Glucosidase Inhibitors: Chemical Structure and Biological Activity. *Tetrahedron* **2006**, *62*, 10277–10302.

(12) Bishop, J. H. V.; Green, R.; Thomas, S. Free-flow Reabsorption of Glucose, Sodium, Osmoles and Water in Rat Proximal Convuluted Tubule. *J. Physiol.* **1979**, *288*, 331–351.

(13) Rajesh, R.; Naren, P.; Vidyasagar, S.; Unnikrishnan; Pandey, S.; Varghese, M.; Gang, S. Sodium Glucose Cotransporter 2 (SGLT2) Inhibitors: A New Sword for the Treatment of Type 2 Diabetes Mellitus. *Int. J. Pharma Sci. Res.* **2010**, *1*, 139–147.

(14) Vallon, V. The Mechanisms and Therapeutic Potential of SGLT2 Inhibitors in Diabetes Mellitus. *Annu. Rev. Med.* **2015**, *66*, 255–270.

(15) Jabbour, S. A.; Goldstein, B. J. Sodium Glucose Co-Transporter 2 Inhibitors: Blocking Renal Tubular Reabsorption of Glucose to Improve Glycaemic Control in Patients with Diabetes. *Int. J. Clin. Pract.* **2008**, *62*, 1279–1284.

(16) Bianchi, L.; Diez-Sampedro, A. A Single Amino Acid Change Converts the Sugar Sensor SGLT3 into a Sugar Transporter. *PLoS One* **2010**, *5*, e10241.

(17) Diez-Sampedro, A.; Hirayama, B. A.; Osswald, C.; Gorboulev, V.; Baumgarten, K.; Volk, C.; Wright, E. M.; Koepsell, H. A Glucose Sensor Hiding in a Family of Transporters. *Proc. Natl. Acad. Sci. U. S. A.* **2003**, *100*, 11753–11758.

(18) Wright, E. M.; Turk, E. The Sodium/Glucose Cotransport Family SLC5. *Pfluegers Arch.* **2004**, *447*, 510–518.

(19) Wright, E. M.; Loo, D. D. F.; Hirayama, B. A. Biology of Human Sodium Glucose Transporters. *Physiol. Rev.* **2011**, *91*, 733–794.

(20) Kalra, S. Sodium Glucose Co-Transporter-2 (SGLT2) Inhibitors: A Review of Their Basic and Clinical Pharmacology. *Diabetes Ther.* **2014**, *5*, 355–366.

(21) Rossetti, L.; Smith, D.; Shulman, G. I.; Papachristou, D.; DeFronzo, R. A. Correction of Hyperglycemia with Phlorizin Normalizes Tissue Sensitivity to Insulin in Diabetic Rats. *J. Clin. Invest.* **1987**, *79*, 1510–1515.

(22) Ehrenkranz, J. R. L.; Lewis, N. G.; Kahn, C. R.; Roth, J. Phlorizin: A Review. *Diabetes/Metab. Res. Rev.* **2005**, *21*, 31–38.

(23) Katsuno, K.; Fujimori, Y.; Takemura, Y.; Hiratochi, M.; Itoh, F.; Komatsu, Y.; Fujikura, H.; Isaji, M. Sergliflozin, a Novel Selective Inhibitor of Low-Affinity Sodium Glucose Cotransporter (SGLT2), Validates the Critical Role of SGLT2 in Renal Glucose Reabsorption and Modulates Plasma Glucose Level. *J. Pharmacol. Exp. Ther.* **2007**, *320*, 323–330.

(24) Oku, A.; Ueta, K.; Arakawa, K.; Ishihara, T.; Nawano, M.; Kuronuma, Y.; Matsumoto, M.; Saito, A.; Tsujihara, K.; Anai, M.; Asano, T.; Kanai, Y.; Endou, H. T-1095, an Inhibitor of Renal Na^+ -Glucose Cotransporters, May Provide a Novel Approach to Treating Diabetes. *Diabetes* **1999**, *48*, 1794–1800.

(25) Powell, D. R.; Smith, M.; Greer, J.; Harris, A.; Zhao, S.; Da Costa, C.; Mseeh, F.; Shadoan, M. K.; Sands, A.; Zambrowicz, B.; Ding, Z.-M. LX4211 Increases Serum Glucagon-Like Peptide 1 and Peptide YY Levels by Reducing Sodium/Glucose Cotransporter 1

(SGLT1)-Mediated Absorption of Intestinal Glucose. *J. Pharmacol. Exp. Ther.* **2013**, *345*, 250–259.

(26) Shibazaki, T.; Tomae, M.; Ishikawa-Takemura, Y.; Fushimi, N.; Itoh, F.; Yamada, M.; Isaji, M. KGA-2727, a Novel Selective Inhibitor of a High-Affinity Sodium Glucose Cotransporter (SGLT1), Exhibits Antidiabetic Efficacy in Rodent Models. *J. Pharmacol. Exp. Ther.* **2012**, *342*, 288–296.

(27) Kojima, N.; Williams, J. M.; Takahashi, T.; Miyata, N.; Roman, R. J. Effects of a New SGLT2 Inhibitor, Luseogliflozin, on Diabetic Nephropathy in T2DN Rats. *J. Pharmacol. Exp. Ther.* **2013**, *345*, 464–472.

(28) Buqui, G. A.; Sy, S. K. B.; Merino-Sanjuan, M.; Gouvea, D. R.; Nixdorf, S. L.; Kimura, E.; Derendorf, H.; Lopes, N. P.; Diniz, A. Characterization of Intestinal Absorption of C-Glycoside Flavonoid Vicenin-2 from *Lychnophora ericoides* Leaves in Rats by Nonlinear Mixed Effects Modeling. *Rev. Bras. Farmacogn.* **2015**, *25*, 212–218.

(29) Pan, X.; Huan, Y.; Shen, Z.; Liu, Z. Synthesis and Biological Evaluation of Novel Tetrahydroisoquinoline-C-Aryl Glucosides as SGLT2 Inhibitors for the Treatment of Type 2 Diabetes. *Eur. J. Med. Chem.* **2016**, *114*, 89–100.

(30) Anderson, S. L. Dapagliflozin Efficacy and Safety: A Perspective Review. *Ther. Adv. Drug Saf.* **2014**, *5*, 242–254.

(31) Kamakura, R.; Son, M. J.; de Beer, D.; Joubert, E.; Miura, Y.; Yagasaki, K. Antidiabetic Effect of Green Rooibos (*Aspalathus linearis*) Extract in Cultured Cells and Type 2 Diabetic Model KK-Ay Mice. *Cytotechnology* **2015**, *67*, 699–710.

(32) Ku, S.-K.; Kwak, S.; Kim, Y.; Bae, J.-S. Aspalathin and Nothofagin from Rooibos (*Aspalathus linearis*) Inhibits High Glucose-Induced Inflammation In Vitro and In Vivo. *Inflammation* **2015**, *38*, 445–455.

(33) Pasetto, P.; Walczak, M. C. A Mitsunobu Route to C-Glycosides. *Tetrahedron* **2009**, *65*, 8468–8477.

(34) Matsumoto, T.; Katsuki, M.; Jona, H.; Suzuki, K. Synthetic Study Toward Vineomycins. Synthesis of C-Aryl Glycoside Sector via Hafnocene Dichloride-Silver Perchlorate-Promoted Tactics. *Tetrahedron Lett.* **1989**, *30*, 6185–6188.

(35) Wellington, K. W.; Benner, S. A. Synthesis of Aryl C-glycosides via the Heck Coupling Reaction. *Nucleosides, Nucleotides Nucleic Acids* **2006**, *25*, 1309–1333.

(36) Koester, D. C.; Leibel, M.; Neufeld, R.; Werz, D. B. A Pd-Catalyzed Approach to (1 \rightarrow 6)-Linked C-Glycosides. *Org. Lett.* **2010**, *12*, 3934–3937.

(37) El Telbani, E.; El Desoky, S.; Hammad, M. A.; Abdel Rahman, A. R. H.; Schmidt, R. R. C-Glycosides of Visnagin Analogs. *Eur. J. Org. Chem.* **1998**, *1998*, 2317–2322.

(38) SanMartin, R.; Tavassoli, B.; Walsh, K. E.; Walter, D. S.; Gallagher, T. Radical-Mediated Synthesis of α -C-Glycosides Based on N-Acyl Galactosamine. *Org. Lett.* **2000**, *2*, 4051–4054.

(39) Matsumoto, T.; Katsuki, M.; Suzuki, K. New Approach to C-Aryl Glycosides Starting from Phenol and Glycosyl Fluoride. Lewis Acid-Catalyzed Rearrangement of O-Glycoside to C-Glycoside. *Tetrahedron Lett.* **1988**, *29*, 6935–6938.

(40) Palmacci, E. R.; Seeberger, P. H. Synthesis of C-Aryl and C-Alkyl Glycosides Using Glycosyl Phosphates. *Org. Lett.* **2001**, *3*, 1547–1550.

(41) dos Santos, R. G.; Jesus, A. R.; Caio, J. M.; Rauter, A. P. Fries-Type Reactions for the C-Glycosylation of Phenols. *Curr. Org. Chem.* **2011**, *15*, 128–148.

(42) Jesus, A. R.; Dias, C.; Matos, A. M.; de Almeida, R. F. M.; Viana, A. S.; Marcelo, F.; Ribeiro, R. T.; Macedo, M. P.; Airoidi, C.; Nicotra, F.; Martins, A.; Cabrita, E. J.; Jimenez-Barbero, J.; Rauter, A. P. Exploiting the Therapeutic Potential of 8- β -D-Glucopyranosylgenistein: Synthesis, Antidiabetic Activity, and Molecular Interaction with Islet Amyloid Polypeptide and Amyloid β -Peptide (1–42). *J. Med. Chem.* **2014**, *57*, 9463–9472.

(43) Baell, J.; Walters, M. A. Chemistry: Chemical Con Artists Foil Drug Discovery. *Nature* **2014**, *513*, 481–483.

(44) Ingolfsson, H. I.; Thakur, P.; Herold, K. F.; Hobart, E. A.; Ramsey, N. B.; Periole, X.; de Jong, D. H.; Zwama, M.; Yilmaz, D.; Hall, K.; Maretzky, T.; Hemmings, H. C.; Blobel, C.; Marrink, S. J.

- Kocer, A.; Sack, J. T.; Andersen, O. S. Phytochemicals Perturb Membranes and Promiscuously Alter Protein Function. *ACS Chem. Biol.* **2014**, *9*, 1788–1798.
- (45) Hillis, W. E.; Inoue, T. Polyphenols of *Nothofagus* Species. II. Heartwood of *Nothofagus fusca*. *Phytochemistry* **1967**, *6*, 59–67.
- (46) Whitmore, F. C.; Pietrusza, E. W.; Sommer, L. H. Organosilicon Compounds. X. Molecular Rearrangements. 10. Hydrogen-Halogen Exchange Reactions of Triethylsilane. New Rearrangement of Neopentyl Chloride. *J. Am. Chem. Soc.* **1947**, *69*, 2108–2110.
- (47) Yepremyan, A.; Salehani, B.; Minehan, T. G. Concise Total Syntheses of Aspalathin and Nothofagin. *Org. Lett.* **2010**, *12*, 1580–1583.
- (48) Zhu, A.; Romero, R.; Petty, H. R. An Enzymatic Fluorimetric Assay for Glucose-6-phosphate: Application in an In Vitro Warburg-Like Effect. *Anal. Biochem.* **2009**, *388*, 97–101.
- (49) Saito, K.; Lee, S.; Shiuchi, T.; Toda, C.; Kamijo, M.; Inagaki-Ohara, K.; Okamoto, S.; Minokoshi, Y. An Enzymatic Photometric Assay for 2-Deoxyglucose Uptake in Insulin-Responsive Tissues and 3T3-L1 Adipocytes. *Anal. Biochem.* **2011**, *412*, 9–17.
- (50) Rawat, P.; Kumar, M.; Rahuja, N.; Srivastava, D. S. L.; Srivastava, A. K.; Maurya, R. Synthesis and Antihyperglycemic Activity of Phenolic C-Glycosides. *Bioorg. Med. Chem. Lett.* **2011**, *21*, 228–233.
- (51) Liu, W.; Wang, H.; Meng, F. In Silico Modeling of Aspalathin and Nothofagin Against SGLT2. *J. Theor. Comput. Chem.* **2015**, *14*, 1550056.
- (52) Pinkofsky, H. B.; Dwyer, D. S.; Bradley, R. J. The Inhibition of GLUT1 Glucose Transport and Cytochalasin B Binding Activity by Tricyclic Antidepressants. *Life Sci.* **1999**, *66*, 271–278.
- (53) Pinkofsky, H. B.; Rampal, A. L.; Cowden, M. A.; Jung, C. Y. Cytochalasin B Binding Proteins in Human Erythrocyte Membranes. Modulation of Glucose Sensitivity by Site Interaction and Partial Solubilization of Binding Activities. *J. Biol. Chem.* **1978**, *253*, 4930–4937.
- (54) Jung, C. Y.; Rampal, A. L. Cytochalasin B Binding Sites and Glucose Transport Carrier in Human Erythrocyte Ghosts. *J. Biol. Chem.* **1977**, *252*, 5456–5463.
- (55) Baell, J. B.; Holloway, G. A. New Substructure Filters for Removal of Pan Assay Interference Compounds (PAINS) from Screening Libraries and for Their Exclusion in Bioassays. *J. Med. Chem.* **2010**, *53*, 2719–2740.
- (56) Lagorce, D.; Sperandio, O.; Baell, J. B.; Miteva, M. A.; Villoutreix, B. O. FAF-Drugs3: A Web Server for Compound Property Calculation and Chemical Library Design. *Nucleic Acids Res.* **2015**, *43*, W200–W207.
- (57) Schmid, N.; Eichenberger, A. P.; Choutko, A.; Riniker, S.; Winger, M.; Mark, A. E.; van Gunsteren, W. F. Definition and Testing of the GROMOS Force-Field Versions 54A7 and 54B7. *Eur. Biophys. J.* **2011**, *40*, 843–856.
- (58) MacCallum, J. L.; Bennett, W. F. D.; Tieleman, D. P. Distribution of Amino Acids in a Lipid Bilayer from Computer Simulations. *Biophys. J.* **2008**, *94*, 3393–3404.
- (59) Abraham, M. J.; Murtola, T.; Schulz, R.; Páll, S.; Smith, J. C.; Hess, B.; Lindahl, E. GROMACS: High Performance Molecular Simulations Through Multi-level Parallelism from Laptops to Supercomputers. *SoftwareX* **2015**, *1–2*, 19–25.
- (60) Hermans, J.; Berendsen, H. J. C.; Van Gunsteren, W. F.; Postma, J. P. M. A Consistent Empirical Potential for Water-Protein Interactions. *Biopolymers* **1984**, *23*, 1513–1518.
- (61) Koziara, K. B.; Stroet, M.; Malde, A. K.; Mark, A. E. Testing and Validation of the Automated Topology Builder (ATB) Version 2.0: Prediction of Hydration Free Enthalpies. *J. Comput.-Aided Mol. Des.* **2014**, *28*, 221–233.
- (62) Tironi, I. G.; Sperb, R.; Smith, P. E.; van Gunsteren, W. F. A Generalized Reaction Field Method for Molecular Dynamics Simulations. *J. Chem. Phys.* **1995**, *102*, 5451–9.
- (63) Hess, B. P-LINCS: A Parallel Linear Constraint Solver for Molecular Simulation. *J. Chem. Theory Comput.* **2008**, *4*, 116–122.
- (64) Miyamoto, S.; Kollman, P. A. SETTLE: An Analytical Version of the SHAKE and RATTLE Algorithm for Rigid Water Models. *J. Comput. Chem.* **1992**, *13*, 952–62.
- (65) Bussi, G.; Donadio, D.; Parrinello, M. Canonical Sampling Through Velocity Rescaling. *J. Chem. Phys.* **2007**, *126*, 014101.
- (66) Parrinello, M.; Rahman, A. Polymorphic Transitions in Single Crystals: A New Molecular Dynamics Method. *J. Appl. Phys.* **1981**, *52*, 7182–7190.
- (67) Hub, J. S.; de Groot, B. L.; van der Spoel, D. g_wham: A Free Weighted Histogram Analysis Implementation Including Robust Error and Autocorrelation Estimates. *J. Chem. Theory Comput.* **2010**, *6*, 3713–3720.